RESEARCH ARTICLE | AUGUST 13 2024

Uncertainty of typhoon extreme wind speeds in Hong Kong integrating the effects of climate change

Special Collection: Flow and Civil Structures

Jiayao Wang (王佳瑶) ; Siqi Cao (曹思奇) ; Runze Zhang (张润泽); Sunwei Li (李孙伟) ; Tim K. T. Tse (谢锦添)

Physics of Fluids 36, 087126 (2024)
https://doi.org/10.1063/5.0220590

Physics of Fluids ARTICLE pubs.aip.org/aip/pof

Uncertainty of typhoon extreme wind speeds in Hong Kong integrating the effects of climate change

Cite as: Phys. Fluids **36**, 087126 (2024); doi: 10.1063/5.0220590
Submitted: 27 May 2024 · Accepted: 24 July 2024 ·
Published Online: 13 August 2024

Jiayao Wang (王佳瑶),[1] Siqi Cao (曹思奇),[2] Runze Zhang (张润泽),[3] Sunwei Li (李孙伟),[4,a)] and Tim K. T. Tse (谢锦添)[2]

AFFILIATIONS

[1]Department of Civil and Environmental Engineering, The Hong Kong Polytechnic University, Kowloon, Hong Kong
[2]Department of Civil and Environmental Engineering, The Hong Kong University of Science and Technology, Clear Water Bay, Kowloon, Hong Kong
[3]China Construction Eighth Engineering Division Co., Ltd. Southwest Branch, Chengdu, Sichuan, China
[4]Institute for Ocean Engineering, Tsinghua Shenzhen International Graduate School, Shenzhen, Guangdong, China

Note: This paper is part of the special topic, Flow and Civil Structures.
[a)]**Author to whom correspondence should be addressed:** li.sunwei@sz.tsinghua.edu.cn

ABSTRACT

To assess the influence of climate change on the estimates of extreme wind speeds induced by typhoons, the present study employs a Monte Carlo simulation approach to forecast the extreme wind speeds in the proximity of Hong Kong when the sea surface temperatures rise as projected by various climate change models according to the Representative Concentration Pathway (RCP) 8.5. In addition, the present study shows the first attempt to quantitatively assess the uncertainty buried in the prediction of the extreme wind speed in association with typhoons taking the rise in sea surface temperatures, and therefore climate change, into consideration. It is found that climate change leads, with high confidence, to the increase in extreme wind speeds brought about by typhoons. From the numerical simulation, it is found that the mean wind speeds associated with typhoons impacting Hong Kong rise from 10.8 m/s (1961–1990) to 12.4 m/s (2051–2080), and the extreme wind speed is 47.5 m/s during 2051–2080 under the RCP 8.5 climate scenario, which is 21.2% higher than that corresponding to the period of 1961–1990. As for the quantification of uncertainties in the extreme wind estimates, the inter-quartile ranges for the sea surface temperatures projected by various climate models in July and October are 9.5% and 8.2% in 2050, respectively, and go up to 9.6% and 9.9% in 2080. The extreme wind speeds with 50 years return period show inter-quartile ranges of 14.2% in 2050, and the value decreases to 12.8% in 2080.

I. INTRODUCTION

Typhoon is one of the most destructive extreme weather events that affect human societies and induce disasters in Northwest Pacific Ocean coastal societies. From 1961 to 2010, the annual direct economic losses caused by typhoons in China were approximately US$3.9 billion,[1] and the annual average casualties were 472.[2] In addition to China, the supertyphoon Parma that occurred in 2009 caused nearly 500 fatalities and an estimated economic loss of up to US$581 million in the Philippines.[3] Typhoon Haiyan of 2013, in addition, caused 5982 deaths in the Leyte Gulf area, with additional infrastructure and agriculture damages reaching up to US$802 million.[4] Furthermore, the estimated direct economic loss in Hong Kong due to typhoon Mangkhut in 2018 was about HK$4.60 billion.[5] In recent years, the positive influence of global warming on typhoon sizes, intensities, and occurrence rates has received growing attention.[6–9] Emanuel,[10] for example, found an increasing destructive trend of tropical cyclones in the western Pacific and Atlantic regions in the past thirty years. Since climate change is considered a major reason for the increase in the observed sea surface temperature (SST) and the sea is the ultimate energy source for a typhoon to generate and to grow, climate change certainly impacts the generation, intensification, and decay of a typhoon. More specifically, climate change is considered to be the reason for the increase in both the number and intensity of typhoons.[11–14] These findings have raised great concern regarding the safety of coastal structures in the future when climate change brings more intensive typhoons to the coastline.[15]

Due to the random nature of extreme weather events, the assessment of hazards associated with typhoons is commonly conducted in a statistical sense. Therefore, either long-term measurements or ample numerical simulation results are required to calculate the hazardous indicators of typhoons for statistical assessments. Concerning the long-term measurements, the anemometers installed in the remote stations are vulnerable under extreme conditions, and hence, insufficient observational data associated with typhoons could lead to inaccurate estimations of typhoon hazards.[16,17] With regard to the numerical simulation results, the Monte Carlo simulation (MCS) is considered a mainstream tool to obtain the required large amount of numerically simulated wind speeds within the typhoon boundary layer and hence is widely accepted by the community.[16,18,19] In the MCS, selective key parameters are randomly drawn based on known probability distributions and then input into a boundary layer wind field model to calculate the wind speed time series at the site of interest. Given the MCS produces a large quantity of wind speed data at a given location under the attacks of typhoons, it has long been used as a supplement to the *in situ* measurements in the assessment of typhoon hazards and to estimate the wind loads for safety evaluation of structures in the typhoon-prone area. Vickery and Twisdale,[20] for instance, obtained the typhoon wind speeds from the MCS along the coastline of the United States and concluded that the design wind speeds suggested by ASCE-7-88 and Batts *et al.*[21] are excessively conservative for the inland strip within 200 km from the coastline. Similar outcomes were obtained by Huang *et al.*[22] and Mudd *et al.*[23] Within this trend, a number of previous studies in fact employed the MCS to estimate wind speeds from virtual typhoons and then to compute the extreme wind speed with various desired return periods.[16,24–27] In summary, the MCS is frequently employed as a supplement to the *in situ* measurements to estimate the extreme wind speeds at the site of interest and then to numerically estimate extremes from the fitted probability distributions, which are commonly used in codifications of wind loads, as well as to provide information for risk and loss assessments.

Given the profound impacts of climate change on various meteorological phenomena, many scholars have suggested to take into consideration the influence of climate change in the MCS of typhoon attacks. For example, Mudd *et al.*[23,28] took the impacts of SSTs on the central pressure of typhoons into consideration in devising the wind field model based on the empirical model proposed by Vickery *et al.*[29] Chu *et al.*[30] improved the Vickery empirical model and revealed the relations between the SST varied in association with climate change and the radius to the maximum wind (RMW), central pressure difference, and latitude of typhoon center. Wang *et al.*[31] demonstrated the impacts of SSTs on the six key parameters defining the size and intensity of the typhoon boundary layer, including the central pressure deficit ΔP, the RMW, and occurrence rate λ. Although the relationships between SST and the key characteristics of typhoon wind field, which emphasize the importance of taking into account climate change in typhoon hazards assessment, are already presented by Wang *et al.*,[31] and a few other previous studies indicate the positive correlations between SST and typhoon intensity and extreme wind speed,[32–34] the uncertainties of such assessments induced by the prediction of future climates have not been investigated. Additionally, many existing studies on SST uncertainty rely solely on observational data[35–37] or are based on scenarios from previous generations of climate models,[38,39] and some previous studies focus only on a single or a limited selection of SST models.[35,40] In contrast, this study utilized the Coupled Model Intercomparison Project Phase 5 (CMIP5) scenarios and considered all available models to comprehensively analyze the uncertainties. Therefore, the inter-model uncertainties can be estimated. Since the forecast of the future climate change pathway, and therefore the future variation in SSTs, is highly uncertain due to the complex social-economic influences and the random nature of the weather system, the study on the uncertainty buried in the assessment of the typhoon hazards in the future due to climate change is necessary.

To quantify the uncertainties buried in the assessment of typhoon hazards in the proximity of Hong Kong under the influence of climate change, the present study investigates both the prediction of extreme wind speeds induced by typhoons and the associated uncertainties via the MCS approach. In fact, the present study is an improvement on the methodology and conclusion from the work of Wang *et al.*[31] with regard to the following:

- The severe climate change scenario with future Greenhouse Gas emission impacts (RCP 8.5) was applied to predict the variations in the typhoon wind field.
- The sensitivity analysis concerning the impact range employed in the MCS is conducted to show the influence of a key component on the prediction of extreme wind speed.
- The uncertainties in the prediction of extreme wind speeds associated are quantified, which helps the evaluation of the typhoon hazards assessments.

In detail, the present study utilizes the Representative Concentration Pathways (RCPs) climate scenario, which excludes any social and economic impact factors and only focuses on the greenhouse gas concentration to quantify the degree of global warming. The projected SSTs under the RCP 8.5 scenario (the most severe case), which was briefed by the Intergovernmental Panel on Climate Change (IPCC) in the fifth Assessment Report (AR5), are regarded as the future large-scale environment for the MCS of typhoons.[41] The present study selects Hong Kong as a case study. On the one hand, Hong Kong is densely populated with high economic values. On the other hand, it is vulnerable to the hazards brought about by typhoons. Both the value and the vulnerability make understanding the influence of climate change on extreme wind conditions in association with typhoons an urgent matter for Hong Kong society.[5,42] In the MCS, the RCP 8.5 scenario stipulates the rise in SST, which in turn leads to the probability distributions for drawing the key parameters defining the movement, sizes, and intensities of typhoons. Afterward, the wind speeds at the site of interest are numerically estimated. In such a process, the sensitivity of a key variable adopted in the MCS, i.e., the typhoon impact range, is numerically investigated. The current study conducts a detailed sensitivity analysis to investigate three potential impact ranges—250, 500, and 1000 km—to determine which provide the most accurate and reliable forecasts for statistical and extreme typhoon wind for Hong Kong. Given the random nature of the weather system, the predictions on the future variations in the large-scale environment are different from different models, even though the general pathway is specified under the RCP 8.5 scenario. Such differences are taken as an indicator showing the uncertainty in the prediction of both the SST and the extreme wind speeds associated with typhoons. Using the SST projected from different models to run the MCS, the present study delivers, to the best of our knowledge, the first

attempt to quantify the uncertainties in forecasting typhoon wind speeds under the influence of climate change.

After the introduction, Sec. II articulates the methodology to simulate the typhoon wind fields under the influence of climate change, including drawing the key parameters from the projected probability distributions, the refined wind field model, and the process for conducting the MCS. During the MCS, the sensitivity of the typhoon impact range is investigated and reported. Section III validates the models to forecast the SST and the refined typhoon wind field model to calculate the boundary layer wind speeds from the known key parameters. After the verification, the results concerning future variations in the typhoon wind speeds and uncertainties buried in the estimates of extreme wind speed in Hong Kong are discussed in Sec. IV. Finally, concluding remarks are given in Sec. V.

II. METHODOLOGY

In the present study, the extreme wind speeds associated with typhoons under the influence of climate change are estimated statistically from a series of MCS. Generally, the MCS procedures are divided into four steps as follows: (1) obtain characteristic typhoon parameters (i.e., translation speed, approach angle, central pressure deficit, the distance of closest approach, and occurrence rate) from the best-track data maintained by the Hong Kong Observatory, which lays the foundation for the formulation of their probability distributions. It should be noted that the RMW is not directly provided by the best-track data and is calculated according to the central pressure deficit in the present study;[43] (2) set up the probabilistic models of each typhoon key parameter based on the observed SSTs; (3) estimate the impacts of the increases in SSTs, due to climate change, on the probability distribution, which drives the refined typhoon wind field model to predict the typhoon wind field in the future; and (4) the wind speeds at the site of interest are accumulated in the process of the MCS, and the extreme wind speeds are statistically estimated by using the peak-over-threshold method, which is introduced in Sec. II D.

Waglan Island ($22°11'N$, $114°18'E$) is located on the southeastern coast of Hong Kong and provides unimpeded exposure to the South China Sea (in Fig. 1). The open surrounding terrain of Waglan Island makes it an ideal site for the Hong Kong Observatory (HKO) to gather typhoon wind field data for meteorological observations and analysis. The long-standing operation of an anemometer, which was installed at an elevation of 83 meters above the ground level and has been continuously capturing wind speed data, ensures that the measurements are representative of the overwater wind speeds that influence typhoon formation and progression and offer invaluable insights for typhoon prediction models and climatological research. The current study adopts the observation of typhoon wind field data at Waglan Island from 1961 to 2020 (60 years) to estimate the relations between SST and predicted typhoon wind field.

A. Climate change

The Assessment Reports are published regularly through the Intergovernmental Panel on Climate Change (IPCC) to provide comprehensive evaluations of climate change.[44–47] The fifth Assessment Report (AR5) presents the past, present, and future climate scenarios, the responsive strategies, and their expected outcomes. AR5 was published in 2014 within the framework of the Coupled Model Intercomparison Project Phase 5.[48] According to AR5, climate change

FIG. 1. The location of Waglan Island.

is "unequivocal," and human activities are the majority cause of the continuous Greenhouse gas emission leading to global warming. The RCP is therefore adopted to quantify the trajectories of global CO_2 concentrations and hence climate change pathway.[41] Four RCPs have been suggested to capture the levels of Greenhouse gas emission and global warming from RCP 2.6 (stringent mitigation scenario which aims to keep global warming likely below 2 °C compared to the pre-industrial era) to RCP 8.5 (high greenhouse gas emission scenario without additional efforts to constrain the emissions). The global surface temperature rise is expected to exceed 2 °C for the RCP 8.5 scenario with high confidence, and it is a rising radiative forcing pathway that goes up to 8.5 W/m^2 by 2100.[41,49] In this study, the most severe climate change scenario, i.e., the RCP 8.5 scenario, is adopted to predict climate change pathway.

Coastal areas are essential for both economic and social development, and the cities located along the coastlines are prone to disasters originating from the sea, such as typhoons.[50] For the scenario of RCP 8.5, a countable number of studies agreed that global warming would increase the SST in the future,[31,51–53] and the global SST is expected to rise 3.4 °C over the 21st contrary in such a scenario.[54] As a result, the intensity and occurring frequency of typhoons affecting Hong Kong could be changed, which deserves a thorough and systematic investigation.[6,55]

B. Typhoon wind field model

The typhoon wind field model employed in the present study to calculate the typhoon boundary layer wind field for the MCS is presented via governing equations shown in Eqs. (1) and (2).[56,57] These equations are simplified from the full-set Navier–Stokes equation for large-scale geophysical flows and are solved using the numerical approach proposed by Meng *et al.*[56] and Huang *et al.*,[57,58]

$$\frac{d\vec{v}_h}{dt} = -\frac{1}{\rho}\vec{\nabla}_h p - f\vec{k}_h \times \vec{v}_h + \vec{F}_h, \tag{1}$$

$$p = \left\{ p_{c0} + \Delta p_0 \exp\left[-\left(\frac{RMW}{r} \right)^B \right] \right\} \left(1 - \frac{gz}{\theta c_p} \right)^{\frac{c_p}{R}}. \quad (2)$$

In Eqs. (1) and (2), $\vec{v}$ is the wind velocity vector, which is calculated by combing the gradient-level wind velocity and friction-induced wind velocity in the boundary layer; ρ is the air density; p denotes the atmospheric pressure; g is the gravitational acceleration; $\vec{k}$ is the unit vector; $\vec{\Omega}$ is the earth's angle speed; $\vec{F}$ is the frictional force; the subscript h means the parameter in the horizontal plane; f is the Coriolis parameter; p_0 is the surface pressure; z is the height above the sea surface; θ is the potential temperature and is assumed to be constant in the present study; c_p is the specific heat capacity of air; R is the ideal gas constant; p_{c0} is the central pressure of a typhoon at the sea surface; Δp_0 is the central pressure deficit; RMW is the maximum radial distance from the typhoon center to the maximum sustainable wind speed; r is the radial distance from the typhoon center; and B is Holland's radial profile parameter. Two boundary conditions, namely, the upper condition corresponding to the free atmosphere and the lower condition corresponding to the underlying terrain, are applied to constrain the wind field model. The governing equations and the boundary conditions lead to a set of analytical solutions calculating the wind velocities within the typhoon boundary layer shown in Eqs. (3)–(6). In Eqs. (3) and (4), $v_{\theta g}$ and v_{rg} are the tangential and radial components of wind speed at the gradient level; c means the translation velocity of the tropical cyclone; and θ_r is the angle between the typhoon translation direction and the vector from the typhoon center to the site of interest. In Eqs. (5) and (6), $v_{\theta f}$ and v_{rf} are friction-induced wind velocity components in the tangential and radial directions at the surface level, and D_1, D_2, ξ, λ, and χ are empirical parameters estimated as suggested by Meng *et al*,[56]

$$v_{\theta g} = \frac{1}{2}(c \sin\theta_r - fr) + \left[\left(\frac{c \sin\theta_r - fr}{2} \right)^2 + \frac{r}{p}\frac{\partial p}{\partial r} \right]^{\frac{1}{2}}, \quad (3)$$

$$v_{rg} = -\frac{1}{r}\int_0^r \frac{\partial v_{\theta g}}{\partial r} dr, \quad (4)$$

$$v_{\theta f} = e^{-\lambda z}[D_1 \cos(\lambda z) + D_2 \sin(\lambda z)], \quad (5)$$

$$v_{rf} = -\xi e^{-\lambda z}[D_2 \cos(\lambda z) - D_1 \sin(\lambda z)]. \quad (6)$$

C. Probability distributions

Based on the wind field model presented in Sec. II B, the wind speeds at a given location can be calculated using the known key parameters as inputs, such as the translation velocity, the approach angle, the central pressure deficit, the RMW, the minimum of closest distance, and occurrence rate. The probability distributions, based on which the pseudo-stochastic parameters are randomly drawn, are determined following a five-step procedure: (1) procure the key parameters from the best-track data maintained by the Hong Kong Observatory and obtain the corresponding observed regional SSTs (i.e., from a radius of 500 km around Hong Kong, by using the linear-interpolation method for horizontal spatial interpolation) from the European Center for Medium-Range Weather Forecasts (ECMWF) ERA5 database using the time stamp as the link. (2) Select a typhoon impact range and estimate the probability distributions as functions of observed SST for the key parameters using the best-track data as samples. (3) The projected SSTs from different climate change models are substituted in the probability distribution models of key parameters defining the wind fields of upcoming typhoons. (4) The key parameters are then randomly drawn from the probability distributions altered by the variational SST as the input to calculate the wind velocities. (5) Based on the predicted wind speeds and directions obtained from the MCS, the statistics of typhoon wind velocities and the extreme wind speeds in the future are estimated together with the quantified uncertainty.

D. Extreme wind speed estimates

The extreme value distribution is adopted in the present study to estimate the extreme wind speed with any given exceedance probability, as shown in Eqs. (7)–(9). In Eq. (7), F_v denotes the probability for the wind speed less than the value of v in one typhoon case; U means the highest wind speed among n typhoon cases. According to the probability theorem, the probability of that the highest wind speed is smaller than value v in τ years is calculated by Eq. (8), whereas the $p(n, \tau)$ is the probability for n typhoons will occur in τ years. In Eq. (9), T_R is the return period and P_E demonstrates the exceedance probability. In 1928, Fisher and Tippett laid the ground for developing various extreme value distribution models [function F in Eqs. (7) and (8)], by proposing the basic probability theory of extreme values.[59] Afterward, Gumbel formulated the generalized extreme value probability density distribution and defined type I, II, and III extreme value asymptotic metric formulas.[60] The peak-over-threshold method is then suggested, in which all data exceeding a given threshold are taken as extreme data to cope with the shortage of sample amount.[61–63] The method of independent storms,[64] which identifies independent storms from continuous wind speed records and takes the maximum values of independent storms to formulate the extreme value samples, is also suggested to deal with the sample shortage. In this study, the peak-over-threshold (POT) method, with the threshold of 20 m/s, is adopted to generate the samples further probability fitting.[24,65,66] More specifically, the simulated wind speeds, from MCS of typhoon wind field, over the threshold are taken to formulate the sample database. The samples are then binned to show the probability distribution of the extreme wind speed in a discrete manner. The generalized Pareto distribution is then fitted to the binned sample, which yields the parameters used to project the extreme wind speed with any given exceedance probability. In the estimation, the return period, equivalent to the conventional exceedance probability, for calculating the extreme wind speed is specified as 50 years following the wind code in Hong Kong. The details about the estimate of the extreme wind value can be found in Refs. 65 and 66 and Eq. (10), where U_R is the R-year return period wind speed; u_0 is the pre-defined minimum threshold wind speed; σ and k are the scale factor and the shape factor from the fitted generalized Pareto distribution function; and λ is the rate of crossing (number per year),

$$F(U < v|n) = (F_v)^n, \quad (7)$$

$$F(U < v, \tau) = \sum_{n=0}^{\infty} F(U < v|n)p(n, \tau), \quad (8)$$

$$T_R(v) = \frac{1}{P_E(v)}, \quad (9)$$

$$U_R = u_0 + \sigma[1 - (\lambda R)^{-k}]/k. \quad (10)$$

E. Sensitivity analysis of the impact range

In the MCS, the statistics, and hence the probability distribution models, of the key parameters describing the typhoon wind field are generally calculated from the observations of historical typhoons moved within the influencing circle of the site of interest. In fact, a circular impact range is set up around the site of interest, and the typhoon track segments intercepting the circular impact range are extracted and analyzed. Three impact ranges of 250, 500, and 1000 km, defined by the radius of the circle, are widely employed in previous studies to obtain the statistics of the key parameters describing typhoons and hurricanes. For example, Vickery *et al.*,[29] Li and Hong,[25] Liu *et al.*,[67] and Wang *et al.*[31] adopted 250 km as the impact range to analyze the statistics of typhoons. Soisuvarn and Oudomying,[68] Fang *et al.*,[69] and Nayak and Takemi,[70] on the other hand, employed 500 km as the impact range for their MCS. Xiao *et al.*,[24] Wu *et al.*,[71] and Duran and Molinari[72] selected 1000 km. The value of the impact range certainly affects the number of records extracted from the best-track database to formulate the probability distribution models. Therefore, a suitable impact range should include enough number of best-track records and produces reliable and realistic statistics for typhoons.[31] To be comprehensive in terms of delivering reliable MCS, a sensitivity analysis of the impact range has been included in the present study.

The three commonly adopted impact ranges (250, 500, and 1000 km) are used to MCS in the present study. A representative observation point—Waglan Island (WGL) in Hong Kong ($22°11'N$, $114°18'E$)—is chosen as the site of interest due to its surrounding terrain features and the quality/quantity of the available wind records. The wind measurements gathered at the WGL weather station are used to evaluate the accuracy and reliability of the MCS results. In formulating the probability distributions for the key parameters, the best-track data and the observed SSTs extracted from the ECMWF ERA5 database are gathered. Given different impact ranges, different probability distributions of the key parameters defining the typhoon boundary layer wind field are generated for the subsequent MCS. Since the MCS produces a large amount of wind speed and direction records, in theory, statistically agreeing with the observations, the comparison of the wind statistics at WGL station calculated based on numerical and observational data reveals both the sensitivity and appropriateness for choosing a certain value as the impact range.

The comparison of wind statistics from MCS results with observed typhoon data is shown in Fig. 2. The observed typhoon wind speeds and directions from the WGL weather station at 90 m from 1993 to 2020 are adopted to calculate the wind statistics shown in Fig. 2. According to Figs. 2(a)–2(e), the largest deviations of the cumulative density function corresponding to the simulated wind speeds from the observational counterparts are 0.07, 0.08, and 0.16 for the radius of 250, 500, and 1000 km, respectively. Moreover, the largest deviations shown in the figure of wind directions are 0.19, 0.09, and 0.08 for impact range 250, 500, and 1000 km, as indicated in Figs. 2(b), 2(d), and 2(f). It can be discerned from the figures that although the MCS can give a statistical simulation of typhoon wind speeds in better agreement with observations when the impact range is 250 km, the accuracy of wind direction results from MCS corresponding to the impact range of 250 km is not satisfactory. With regard to the impact range of 1000 km, the wind direction statistics from the MCS are in better agreement with the observation data, while the wind speed comparison presents a significant difference. Therefore, 500 km is determined as the impact range in this study since it leads to acceptable statistical estimates of both wind speeds and directions.

III. MODEL VALIDATION

The Coupled Model Intercomparison Project (CMIP) aims to coordinate the comprehensive global climate models, which adopt different schemes in the simulation and hence yield a wide range of outputs to help researchers and policymakers to understand climate variability.[73] In the present study, the historical and projected SSTs are extracted from Earth System Models of the CMIP, as shown in Table I. The SSTs from different models are averaged to reduce possible model errors. For the period from 1961 to 2005, the ensemble mean of all 18 models is utilized, as all models extend at least until 2005 (with the exception of FGOALS-s2, which ends in 2004). For the period extending beyond 2005, the ensemble mean of only those models that are available up to their respective end years is adopted. The monthly SSTs from the models during 1961–2020 under the RCP historical condition are used to compare with the re-analysis SST obtained from the ECMWF ERA5 database to validate the climate change models utilized in the present study. Since the re-analysis data provided by the ERA5 database integrated the observations available from the weather stations worldwide, it is regarded as reliable and hence serves as the comparison criteria. The annual mean SSTs extracted from the re-analysis data of the ERA5 database, averaged model outputs under the RCP historical condition and within the RCP 8.5, are shown in Fig. 3. A similar increase trend can be found for both re-analysis data from the EAR 5 database and the averaged model output under the RCP historical condition. The mean values for the SSTs corresponding to the re-analysis data and model estimates are 24.26 and 24.82 °C, respectively. The model output SST in the RCP 8.5, on the other hand, indicates a noticeable increase trend compared to the historical variation. The mean SST goes up to 26.81 °C, which increases by 2.55 °C (10.51%) compared to the mean ERA5 re-analysis SST and raises around 2 °C (8.02%) compared to the mean RCP historical SST.

IV. EXTREME WIND SPEEDS AND THE ASSOCIATED UNCERTAINTY

Following the methodology articulated in Sec. II, the MCS is conducted to predict the extreme wind speeds at the WGL station in Hong Kong when the world is developing in the pathway of RCP 8.5. More specifically, the probability distributions of the key parameters describing the typhoon boundary layer wind field are projected according to the SSTs projected by various global climate models. Afterward, the wind velocity at the site of interest is calculated based on the typhoon boundary layer wind field model using the input parameter randomly drawn from the projected probability distributions. Repeating such a process following the MCS philosophy, the wind speeds and direction simulation results are accumulated to predict the extreme wind speed. Given various global models shows different predictions on SSTs, the uncertainty of the extreme wind predictions, induced by complexity of the climate change forecasts, is quantitatively assessed in addition to the uncertainty naturally induced by the MCS.

A. Predicted extreme typhoon wind

The distributions of wind speeds and directions from the MCS corresponding to the RCP 8.5 and the historical scenario are compared in Fig. 4. More specifically, the mean SSTs calculated by averaging 17

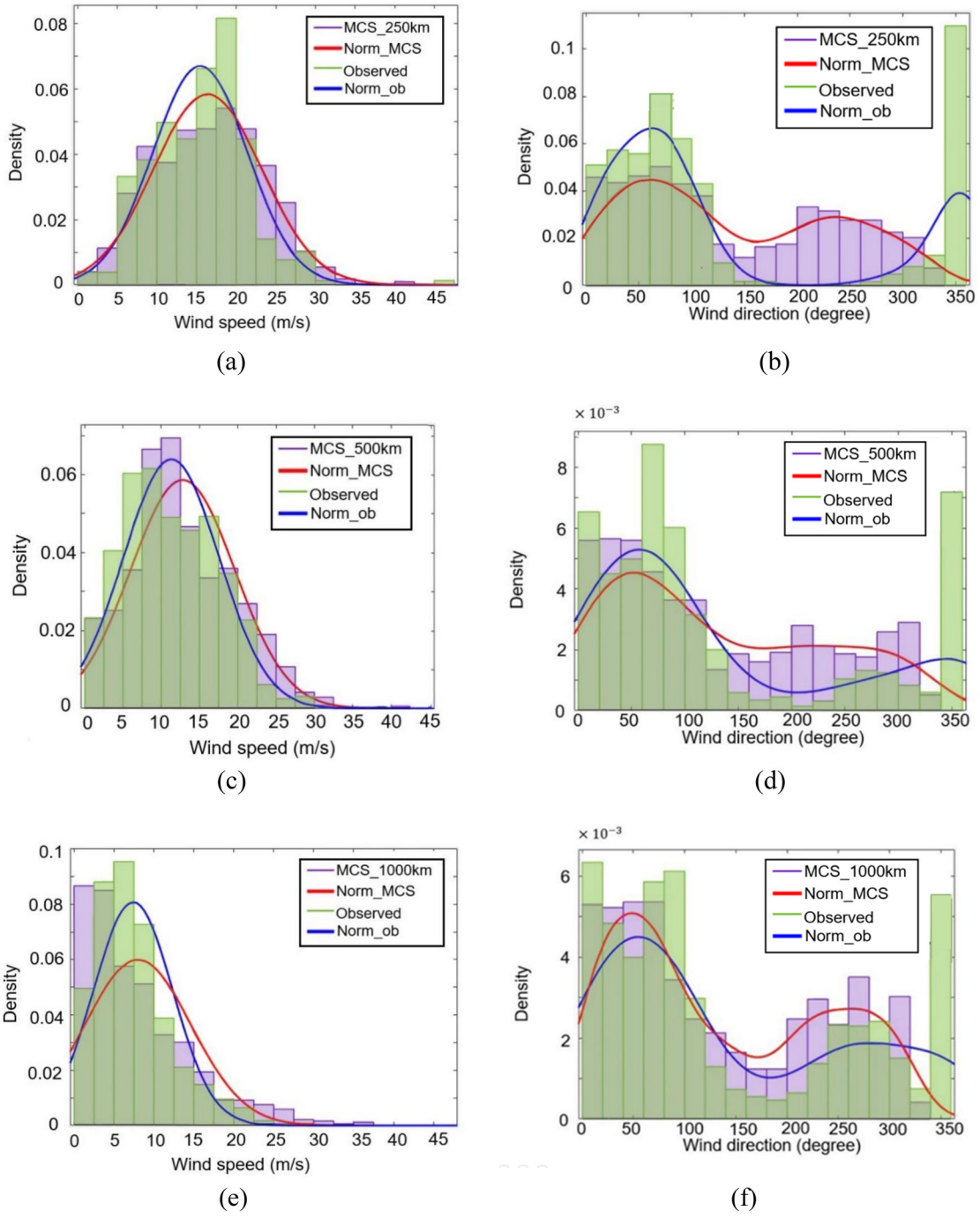

FIG. 2. Sensitivity analysis for three impact ranges. "MCS" means the wind speeds or directions generated by the MCS, and "observed" means the wind field extracted from the WGL weather station during 1993–2020. (a), (c), and (e) The wind speeds at 250, 500, and 1000 km, respectively; (b), (d), and (f) The wind directions at 250, 500, and 1000 km, respectively.

climate model outputs during 2021–2050 and 2051–2080 are used to formulate the probability distributions of the key parameters, which in turn leads to the prediction of the probability distributions of wind speeds and directions in Hong Kong. It is noted that the raw distributions are fitted to the normal distribution model before the comparison shown in the figure for better illustration.

It is observed from Fig. 4(a) that the predicted wind speed increases steadily compared to the historical typhoon wind speed. The

TABLE I. Monthly SST availability.

Model name	RCP his	RCP 8.5
ACCESS1-0	1961–2020	2021–2080
bcc-csm1-1	1961–2012	2021–2080
CanCM4	1961–2012	—
CanESM2	1961–2012	2021–2080
CCSM4	—	2021–2080
CESM1	1961–2005	2021–2080
CSIRO-Mk3-6-0	1961–2012	2021–2080
EC-EARTH	1961–2005	2021–2080
FGOALS-s2	1961–2004	2021–2080
FIO-ESM	1961–2005	2021–2080
GISS-E2-H	1961–2012	2021–2080
HadCM3	1961–2005	—
HadGEM2-ES	1961–2019	2021–2080
INM-CM4	1961–2005	2021–2080
IPSL-CM5A-LR	1961–2005	2021–2080
MIROC-ESM	1961–2005	2021–2080
MPI-ESM-LR	1961–2005	2021–2080
MRI-CGCM3	1961–2012	2021–2080
NorESM1-M	1961–2012	2021–2080
Total model number	18	17

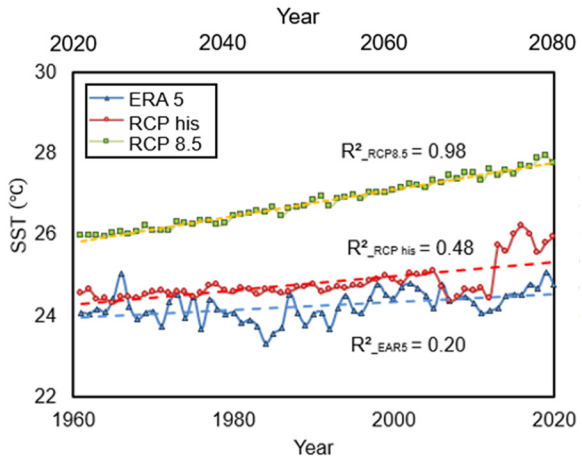

FIG. 3. Annual SSTs from ECMWF ERA5, RCP historical, and RCP 8.5, respectively, where "ERA 5" represents the data obtained from the ECMWF ERA5 and "RCP his" means RCP historical condition.

wind speeds corresponding to the peaks of the distributions are 10.8, 10.9, 12.1, and 12.4 m/s, respectively, for the different periods, as indicated in the figure. Furthermore, the extreme wind speeds with a 50-year return period corresponding to historical periods of 1961–1990 and 1991–2020 are 39.2 and 41.5 m/s, showing an increment of 5.9%. The extreme wind speeds corresponding to the future periods of 2021–2050 and 2051–2080 are 44.3 and 47.5 m/s (an increment of 7.3%). A potential explanation for the observed positive correlation between climate change—indicated as a rise in SST—and the extreme wind speeds induced by typhoons is the role of warmer SSTs in storm dynamics. Higher SSTs provide additional energy and create more favorable conditions for storm development and intensification. Specifically, increased SSTs enhance the enthalpy transfer from the ocean to the atmosphere. This is crucial as it supplies the latent heat energy necessary for the development and intensification of typhoons, thereby increasing their potential for higher wind speeds. Therefore, the increases in SST indeed increase the hazards associated with typhoons.[6,74,75] As indicated in Fig. 4(b), the bi-normal distribution could be adopted to describe the probability distributions of wind directions. It is discerned from the figure that two peaks are shifted with increasing SSTs. More specifically, the first peak shifts from 62.5° to 50° for the first three periods. A slight increase in wind directions, on the other hand, has been found during 2051–2080, and the peak moves backward to 58°. For the second peak shown in Fig. 4(b), a steady decrease trend is found, as the peak move from 275° to 258.3° except for the period of 1991–2020. In summary, under the influence of growing SSTs, the wind directions associated with typhoons generally shift counterclockwise. Such changes may induce severe potential economic losses and even casualties in the densely populated metropolitan areas of Hong Kong because the Kowloon and Hong Kong Island areas are located at SW, W, and SE. Furthermore, the alteration in wind directions may further induce threats to another populated area, i.e., Guangdong Province, which is located along the Southeast coastline of China and to the North of Hong Kong. Therefore, the climate change effects cannot be ignored when estimating extreme winds induced by typhoons in the proximity of Hong Kong.

B. Quantification of uncertainties

The wind-resistant designs of both onshore and offshore structures should take into consideration the extreme wind speeds associated with typhoons in the typhoon-prone region. More specifically, the extreme wind speed with a specific return period is commonly taken as the necessary input to assess the safety of structures. Hence, the strong winds brought about by typhoons play a key role in the structural design and also in the urban planning in the typhoon-prone areas.[76] The uncertainties in the estimates of extreme wind speeds are therefore kin to the safety and development of the costal society. With the help of various global climate models to forecast SSTs, the uncertainty associated with the extreme wind estimates is investigated in the present study. In the present study, the uncertainty originated from either the predictions of the SSTs, or the MCS itself. Therefore, the uncertainty quantification is divided into the analysis concerning the SST predictions and the ultimate uncertainty reflected in the estimate of the extreme wind speed.

1. Uncertainties in the predictions of future SSTs

As shown in Table I, 17 different global climate models are adopted in this study to predict the SSTs for further use by the MCS. It is noted that different global climate models employed various schemes for the predictions of future variations in not only SSTs but also other meteorology variables. Hence, the collections of the SST predictions generated by different global climate models show, to a certain degree, the uncertainty contained in the forecasts concerning the future variations in meteorological variables. Specifically, the typhoon

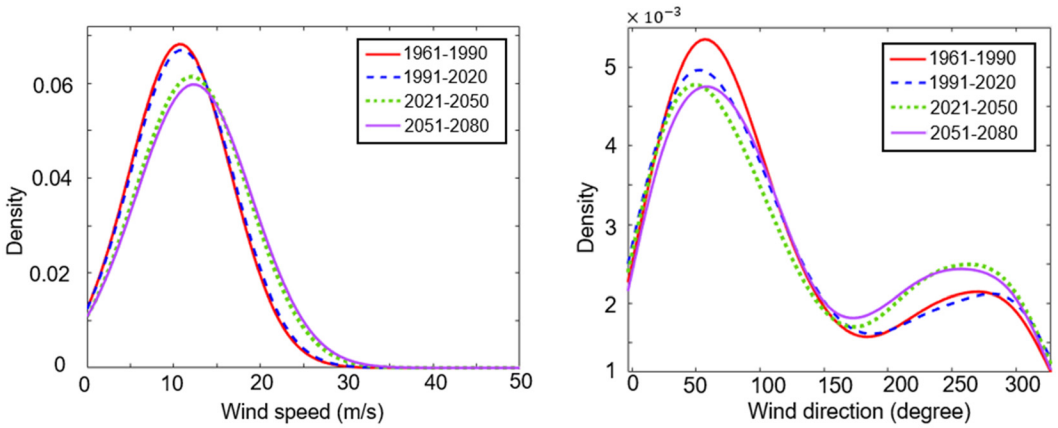

FIG. 4. Comparing the wind statistics corresponding to the previous periods from 1961 to 2020 (total 60 years) with predicted wind speed and direction from 2021 to 2080 (total 60 years) at the WGL station, where the "1961–1990" and "1991–2020" represent the RCP historical condition, while "2021–2050" and "2051–2080" means the predicted value at severe climate change scenario (RCP 8.5). (a) Wind speed and (b) wind direction.

season typically lasts from July to October in Hong Kong.[77–79] Therefore, the future variations in SSTs projected by 17 different climate models during the summer (July) and autumn (October) seasons in 2050 and 2080 are employed to quantify the uncertainties.

The box plots showing the SSTs projected by the 17 different climate models as samples within the pathway of RCP 8.5 in July and October of 2050 and 2080 are given in Fig. 5. From the figure, the average SST in July corresponding to 2050 is 29.2 °C, which is around 1.4 °C lower than the average SST corresponding to 2080. The average SSTs in October in 2050 and 2080 are 28.4 and 29.2 °C, respectively. The inter-quartile ranges (difference between the lower quartile and the upper quartile) of SSTs among climate model predictions corresponding to 2050 are 9.5% ($\Delta = 2.6$ °C) and 8.2% ($\Delta = 2.2$ °C) for July and October. However, the differences between the minimum and the maximum predictions of SST are up to 31.3% ($\Delta = 7.8$ °C) and 33.2% ($\Delta = 7.9$ °C). Similar patterns can be found for 2080, where the inter-quartile ranges are 9.6% ($\Delta = 2.8$ °C) and 9.9% ($\Delta = 2.8$ °C). The maximum–minimum difference goes up to 30.8% ($\Delta = 7.9$ °C) and 31.4% ($\Delta = 7.7$ °C).

2. Uncertainties in the predictions of extreme wind speeds

In the MCS, the uncertainty could be introduced, in addition to the uncertainty in the SST predictions, by the random draw of the key parameters describing the typhoon boundary layer wind field. The present study analyzes the uncertainty for the ultimate estimate of extreme wind speeds in addition to the SST prediction. In detail, the different predictions on the future variations in SSTs from different climate models are used to provide the key parameters necessary for the MCS. Figure 6 shows the statistics of the extreme wind speeds estimated according to different predictions on the future variations in SSTs. The figure shows normal distributions fitted to the samples of 17 different estimates of the extreme wind speeds, and the box plots indicate the variations in the estimates. From Fig. 6(a), it is observed that the mean, calculated according to the fitted normal distribution model, of estimated extreme wind speeds in 2050 and 2080 is 50.0 and 52.7 m/s, respectively. Figure 6(b) illustrates, on the other hand, the inter-quartile range of extreme wind speeds in 2050 is 14.2% ($\Delta = 6.6$ m/s),

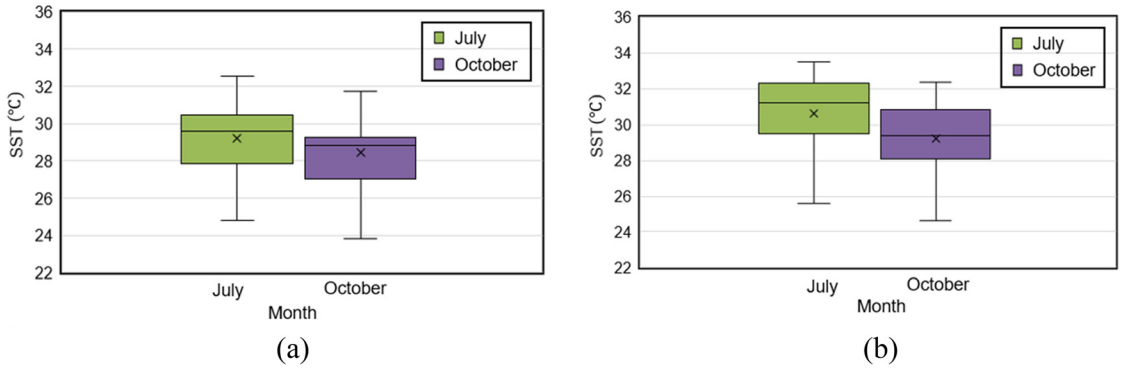

FIG. 5. Box plots of SST obtained from 17 models within the RCP 8.5 scenario in (a) 2050 and (b) 2080, respectively.

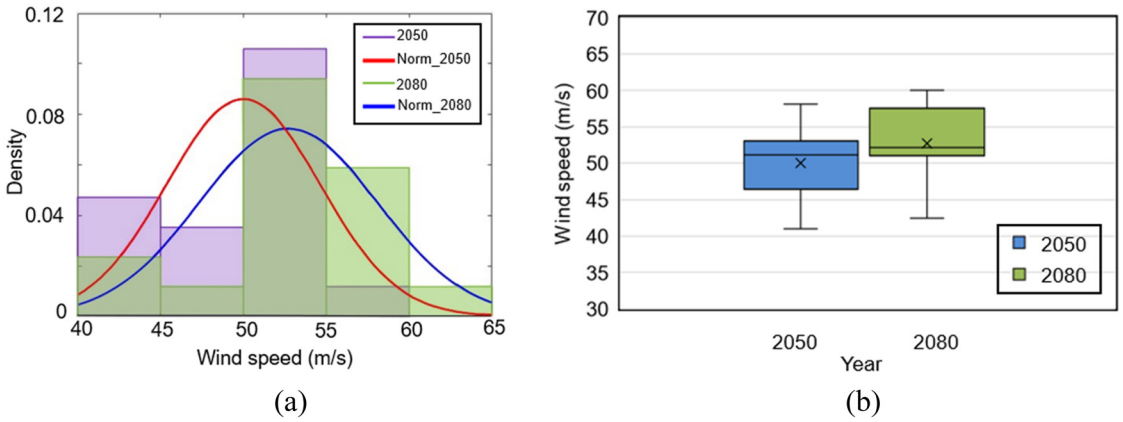

FIG. 6. Extreme wind speeds from 17 SST models within RCP 8.5 scenario at Hong Kong in 2050 and 2080. (a) Extreme winds among 17 SST models and (b) extreme winds among 17 SST models.

and the maximum–minimum difference goes up to 42.1% ($\Delta = 17.2$ m/s). Similar results are observed for the box plot corresponding to 2080, where the inter-quartile range is 12.8% ($\Delta = 6.5$ m/s), and the maximum–minimum difference goes up to 41.7% ($\Delta = 17.7$ m/s). Compared to the discrepancies among the SSTs projected by different global climate models, it is found that the MCS, which includes randomness in nature, increases the uncertainty brought about by the SST forecasts. Specifically, the inter-quartile ranges in 2050 and 2080 of extreme winds (14.2% and 12.8%) are increased from the values corresponding to the SST predictions (9.5% and 8.2% in July and October for 2050 and 9.6% and 9.9% in July and October for 2080). As for the maximum–minimum difference, a clear increment is found for both periods (42.1% compared to 31.3% and 33.2% in 2050 and 41.7% compared to 30.8% and 31.4% in 2080).

3. Discussion on the uncertainties

It is found from the Figs. 5 and 6 that the uncertainties in the predictions of SSTs and the extreme wind speeds are similar for the years of 2050 and 2080. In fact, the inter-quartile ranges corresponding to the predictions at 2050 and 2080 are close to 9% and 13% for SSTs and extreme wind speeds, respectively. Such a finding implies that the uncertainty for the estimates of extreme winds is not increasing with time as one naturally expected. In other words, different climate change models present a consistent and steady prediction on the future variations in SSTs, which in turn leads to steady estimates of extreme wind speeds. Such a finding is also revealed from the maximum–minimum differences corresponding to the predictions for 2050 and 2080, which indicates that almost all the climate change models employed in the present study show steady predictions for the period until 2080. It should be acknowledged that such a feature could be a drawback for the uncertainty analysis as the climate model itself does not take full consideration of the randomness in the meteorological system.

In addition, it is found from the MCS enlarges the uncertainty induced by the SST prediction by a factor of 1.3–1.5. Therefore, the MCS and the extreme value estimation only marginally increases the uncertainty of the prediction, and the uncertainty in the prediction of the extreme wind speeds is majorly induced by the uncertainty for the SST prediction. Since the statistical behavior of the typhoon boundary layer wind field model has been verified, it suggests that the prediction of the extreme wind speed can be improved once the prediction on the SST is more reliable.

Last but not least, the uncertainty for the prediction on the extreme wind speeds at 2080 reduced compared to the prediction at 2050 even though the uncertainty for the SST prediction increases for the same period. This odd discovery implies that the increases in SSTs could reduce the uncertainty in the modeling the typhoon boundary layer wind field and in the extreme value analysis. In other words, there is a limit for the extreme wind speeds estimated from the MCS when the SST is input to stipulate the probability distributions of the key parameters defining the typhoon boundary layer wind field, and the increase in SSTs brings the prediction of the extreme wind speed up to such a limit. Consequently, along with the global warming exacerbate, different models could generally agree on the resulting extreme wind condition.

V. CONCLUDING REMARKS

Since typhoons bring the most severe threats to both the safety and development of society in the Southeast coastline of China and other coastal areas, the hazards associated with typhoons have been a topic for academic research for a relatively long time. In investigating typhoon hazards, the MCS plays a significant role as long-term observations, which are acquired from costly measurement campaigns, are too rare to estimate the extreme wind brought about by typhoons. As for the MCS currently employed to estimate the extreme wind speed in association with typhoons, (a) the widely acknowledged climate change effect is yet considered in the simulation and (b) the uncertainties buried in the estimates are not quantified to show the reliability for the results. The present study targets the above-mentioned two shortcomings and includes the predictions of future SST variations from different global climate models within the climate change pathway of RCP 8.5 in the MCS to assess the uncertainty in the estimates of the extreme wind speeds in Hong Kong.

From the MCS results, it is found that the mean wind speeds associated with typhoons impacting Hong Kong rise from 10.8 m/s (1961–1990) to 12.4 m/s (2051–2080), and the extreme wind speed is

47.5 m/s during 2051–2080 under the RCP 8.5 climate scenario, which is 21.21% higher than that corresponding to the period of 1961–1990. Furthermore, the wind directions from the MCS illustrate a general shift in the counterclockwise direction compared to historical wind data. In conclusion, the constant increase in typhoon wind speeds and changes in the wind directions demonstrate that climate change may lead to more severe damages and losses due to typhoons in Hong Kong or even impact the Southeast of China (i.e., Guangdong Province).

Furthermore, the differences in SSTs from various climate models are used to assess the uncertainties in the estimates of extreme wind speeds based on the MCS results. The inter-quartile ranges (difference between lower quartile and upper quartile) of SSTs from various climate models are 9.5% and 8.2% in July and October of 2050, and the maximum–minimum differences go up to 31.3% and 33.2%. In 2080, the inter-quartile ranges of projected SSTs in July and October are 9.6% and 9.9%, while the maximum–minimum differences are 30.8% and 31.4%. As the MCS introduces additional uncertainties as pseudo-stochastic parameters are input, the ultimate uncertainty in the extreme wind speed estimates is investigated. In 2050, the inter-quartile range of extreme wind speeds estimated using different SST predictions is 14.2%, and the maximum–minimum difference for extreme winds is 42.1%. Similar results are shown for extreme wind speed estimates in 2080, where the inter-quartile range is 12.8%, and the maximum–minimum difference goes up to 41.7%.

It should be noted that the uncertainty considered in the present study originated either from the global climate model in predicting the future variation in SSTs, or from the randomness naturally contained in the MCS. It is noted that the mechanism for various factors to influence the uncertainty in the rising SST is not discussed in the present study, and therefore preclude the development of any theoretical/analytical models to explain the uncertainty in the projected SST. However, it is crucial to understand various social, economic, and natural factors leading to the rising SST. More importantly, the mechanisms for various factors to contribute the uncertainty in the project SST should be the discerned, and therefore is the topic for our future study. While this study provides a comprehensive analysis of climate model uncertainties under a specific emission scenario, it does not extend to exploring scenario uncertainty across different RCPs such as RCP 2.6, 4.5, and 6.0. The uncertainty connected with the wind field modeling is another, and maybe more important, the source of the uncertainty in the ultimate estimate of the extreme wind speeds. However, an investigation on the uncertainty of the wind field modeling requires a large number of measurements spread out in the typhoon wind field, to which the modeled wind speed could be compared and the uncertainty could be assessed. Future studies employing the aircraft and dropsonde measurements in the typhoon wind field provided by the Hong Kong Observatory are undertaken to address this shortage.

ACKNOWLEDGMENTS

The work described in this article was supported by the grants from Guangdong Basic and Applied Basic Research Foundation (Project No. 2022B1515130006). The authors acknowledge the support from the Tsinghua Shenzhen International Graduate School-Shenzhen Pengrui Young Faculty Program of Shenzhen Pengrui Foundation. The numerical computations reported in the manuscript were partially performed at the Hefei Advanced Computing Center.

AUTHOR DECLARATIONS

Conflict of Interest

The authors have no conflicts to disclose.

Author Contributions

Jiayao Wang: Data curation (equal); Validation (equal); Visualization (equal); Writing – original draft (equal); Writing – review & editing (equal). **Siqi Cao:** Methodology (equal); Writing – review & editing (equal). **Runze Zhang:** Visualization (equal); Writing – review & editing (equal). **Sunwei Li:** Funding acquisition (equal); Methodology (equal); Supervision (equal); Writing – review & editing (equal). **Tim K. T. Tse:** Supervision (equal).

DATA AVAILABILITY

The data that support the findings of this study are available from the corresponding author upon reasonable request.

REFERENCES

[1]L. Bakkensen, "The impact of climate and socioeconomic change on typhoon losses in China," CMCC Research Paper 204 (2013).
[2]H. Lam, M. H. Kok, and K. K. Y. Shum, "Benefits from typhoons—The Hong Kong perspective," Weather **67**(1), 16–21 (2012).
[3]Y. A. Liou and R. S. Pandey, "Interactions between typhoons Parma and Melor (2009) in North West Pacific Ocean," Weather Clim. Extremes **29**, 100272 (2020).
[4]N. Mori, M. Kato, S. Kim, H. Mase, Y. Shibutani, T. Takemi *et al.*, "Local amplification of storm surge by Super Typhoon Haiyan in Leyte Gulf," Geophys. Res. Lett. **41**(14), 5106–5113, https://doi.org/10.1002/2014GL060689 (2014).
[5]C. W. Choy, M. C. Wu, and T. C. Lee, "Assessment of the damages and direct economic loss in Hong Kong due to Super Typhoon Mangkhut in 2018," Trop. Cyclone Res. Rev. **9**(4), 193–205 (2020).
[6]T. R. Knutson, J. J. Sirutis, S. T. Garner, G. A. Vecchi, and I. M. Held, "Simulated reduction in Atlantic hurricane frequency under twenty-first-century warming conditions," Nat. Geosci. **1**(6), 359–364 (2008).
[7]G. J. Holland and C. L. Bruyère, "Recent intense hurricane response to global climate change," Clim. Dyn. **42**(3), 617–627 (2014).
[8]M. E. Mann and K. A. Emanuel, "Atlantic hurricane trends linked to climate change," EoS. Trans. AGU **87**(24), 233–241 (2006).
[9]J. Y. Tu, C. Chou, and P. S. Chu, "The abrupt shift of typhoon activity in the vicinity of Taiwan and its association with western North Pacific–East Asian climate change," J. Clim. **22**(13), 3617–3628 (2009).
[10]K. Emanuel, "Increasing destructiveness of tropical cyclones over the past 30 years," Nature **436**(7051), 686–688 (2005).
[11]M. Zhao, I. M. Held, and G. A. Vecchi, "Retrospective forecasts of the hurricane season using a global atmospheric model assuming persistence of SST anomalies," Mon. Weather Rev. **138**(10), 3858–3868 (2010).
[12]I. Takayabu, K. Hibino, H. Sasaki, H. Shiogama, N. Mori, Y. Shibutani *et al.*, "Climate change effects on the worst-case storm surge: A case study of Typhoon Haiyan," Environ. Res. Lett. **10**(6), 064011 (2015).
[13]H. Murakami, E. Levin, T. Delworth, R. Gudgel, and P.-C. Hsu, "Dominant effect of relative tropical Atlantic warming on major hurricane occurrence," Science **362**(6416), 794–799 (2018).
[14]J. C. Trepanier, "North Atlantic hurricane winds in warmer than normal seas," Atmosphere **11**(3), 293 (2020).
[15]K. Tsuboki, M. K. Yoshioka, T. Shinoda, M. Kato, S. Kanada, and A. Kitoh, "Future increase of supertyphoon intensity associated with climate change,"

Geophys. Res. Lett. **42**(2), 646–652, https://doi.org/10.1002/2014GL061793 (2015).
[16]Y. Guo, Y. Hou, and P. Qi, "Analysis of typhoon wind hazard in Shenzhen City by Monte-Carlo simulation," J. Oceanol. Limnol. **37**(6), 1994–2013 (2019).
[17]J. Wang, K. T. Tse, and S. W. Li, "Integrating the effects of climate change using representative concentration pathways into typhoon wind field in Hong Kong," in 8th European African Conference on Wind Engineering, Bucharest, Romania, 20–23 September 2022.
[18]L. Gomes and B. Vickery, "Extreme wind speeds in mixed wind climates," J. Wind Eng. Ind. Aerodyn. **2**(4), 331–344 (1978).
[19]T. Ishihara and A. Yamaguchi, "Prediction of the extreme wind speed in the mixed climate region by using Monte Carlo simulation and measure-correlate-predict method," Wind Energy **18**(1), 171–186 (2015).
[20]P. J. Vickery and L. A. Twisdale, "Prediction of hurricane wind speeds in the United States," J. Struct. Eng. **121**(11), 1691–1699 (1995).
[21]M. E. Batts, E. Simiu, and L. R. Russell, "Hurricane wind speeds in the United States," J. Struct. Div. **106**(10), 2001–2016 (1980).
[22]Z. Huang, D. V. Rosowsky, and P. R. Sparks, "Long-term hurricane risk assessment and expected damage to residential structures," Reliab. Eng. Syst. Saf. **74**(3), 239–249 (2001).
[23]L. Mudd, Y. Wang, C. Letchford, and D. Rosowsky, "Hurricane wind hazard assessment for a rapidly warming climate scenario," J. Wind Eng. Ind. Aerodyn. **133**, 242–249 (2014).
[24]Y. F. Xiao, Z. D. Duan, Y. Q. Xiao, J. P. Ou, L. Chang, and Q. S. Li, "Typhoon wind hazard analysis for southeast China coastal regions," Struct. Saf. **33**(4–5), 286–295 (2011).
[25]S. Li and H. Hong, "Use of historical best track data to estimate typhoon wind hazard at selected sites in China," Nat. Hazards **76**(2), 1395–1414 (2015).
[26]Z. Yan, B. Liang, G. Wu, S. Wang, and P. Li, "Ultra-long return level estimation of extreme wind speed based on the deductive method," Ocean Eng. **197**, 106900 (2020).
[27]M. Huang, Q. Wang, Q. Li, R. Jing, N. Lin, and L. Wang, "Typhoon wind hazard estimation by full-track simulation with various wind intensity models," J. Wind Eng. Ind. Aerodyn. **218**, 104792 (2021).
[28]L. Mudd, Y. Wang, C. Letchford, and D. Rosowsky, "Assessing climate change impact on the U.S. East Coast hurricane hazard: Temperature, frequency, and track," Nat. Hazard Rev. **15**(3), 04014001 (2014).
[29]P. J. Vickery, P. F. Skerlj, and L. A. Twisdale, "Simulation of hurricane risk in the US using empirical track model," J. Struct. Eng. **126**(10), 1222–1237 (2000).
[30]X. Chu, W. Cui, L. Zhao, S. Cao, and Y. Ge, "Probabilistic flutter analysis of a long-span bridge in typhoon-prone regions considering climate change and structural deterioration," J. Wind Eng. Ind. Aerodyn. **215**, 104701 (2021).
[31]J. Wang, K. T. Tse, S. Li, and J. C. Fung, "Prediction of the typhoon wind field in Hong Kong: Integrating the effects of climate change using the Shared Socioeconomic Pathways," Clim. Dyn. **59**(7–8), 2311–2329 (2022).
[32]L. R. Schade, "Tropical cyclone intensity and sea surface temperature," J. Atmos. Sci. **57**(18), 3122–3130 (2000).
[33]S. L. Lavender, R. K. Hoeke, and D. J. Abbs, "The influence of sea surface temperature on the intensity and associated storm surge of tropical cyclone Yasi: A sensitivity study," Nat. Hazards Earth Syst. Sci. **18**(3), 795–805 (2018).
[34]J.-p. Yuan and J. Jiang, "The relationships between tropical cyclone tracks and local SST over the western north pacific," J. Trop. Meteorol. **17**(2), 120 (2011).
[35]J. J. Freer, J. C. Partridge, G. A. Tarling, M. A. Collins, and M. J. Genner, "Predicting ecological responses in a changing ocean: The effects of future climate uncertainty," Mar. Biol. **165**, 7 (2018).
[36]J. J. Kennedy, "A review of uncertainty in in situ measurements and data sets of sea surface temperature," Rev. Geophys. **52**(1), 1–32, https://doi.org/10.1002/2013RG000434 (2014).
[37]J. J. Kennedy, N. A. Rayner, R. O. Smith, D. E. Parker, and M. Saunby, "Reassessing biases and other uncertainties in sea surface temperature observations measured in situ since 1850: 2. Biases and homogenization," J. Geophys. Res.: Atoms. **116**(D14), https://doi.org/10.1029/2010JD015218 (2011).
[38]Y. Yara, M. Fujii, H. Yamano, and Y. Yamanaka, "Projected coral bleaching in response to future sea surface temperature rises and the uncertainties among climate models," Hydrobiologia **733**, 19–29 (2014).
[39]T. Ose and O. Arakawa, "Uncertainty of future precipitation change due to global warming associated with sea surface temperature change in the tropical Pacific," J. Meteorol. Soc. Jpn. **89**(5), 539–552 (2011).
[40]H.-N. Cheung, N. Keenlyside, T. Koenigk, S. Yang, T. Tian, Z. Xu *et al.*, "Assessing the influence of sea surface temperature and arctic sea ice cover on the uncertainty in the boreal winter future climate projections," Clim. Dyn. **59**(1), 433–454 (2022).
[41]K. B. Tokarska and N. P. Gillett, "Cumulative carbon emissions budgets consistent with 1.5 °C global warming," Nat. Clim. Change **8**, 296–299 (2018).
[42]T. Sim, D. Wang, and Z. Han, "Assessing the disaster resilience of megacities: The case of Hong Kong," Sustainability **10**(4), 1137 (2018).
[43]Y. Xiao, Y. Xiao, and Z. Duan, "The typhoon wind hazard analysis in Hong Kong of China with the new formula for Holland B parameter and the CE wind field model," in The Seventh Asia-Pacific Conference on Wind Engineering, Taipei, Taiwan, 2009.
[44]R. K. Pachauri, M. R. Allen, V. R. Barros, J. Broome, W. Cramer, R. Christ *et al.*, *Climate Change 2014: Synthesis Report, Contribution of Working Groups I, II and III to the Fifth Assessment Report of the Intergovernmental Panel on Climate Change* (IPCC, 2014).
[45]M. D. Mastrandrea, K. J. Mach, G.-K. Plattner, O. Edenhofer, T. F. Stocker, C. B. Field *et al.*, "The IPCC AR5 guidance note on consistent treatment of uncertainties: A common approach across the working groups," Clim. Change **108**(4), 675–691 (2011).
[46]A. Revi, D. Satterthwaite, F. Aragón-Durand, J. Corfee-Morlot, R. B. Kiunsi, M. Pelling *et al.*, "Towards transformative adaptation in cities: The IPCC's fifth assessment," Environ. Urbanization **26**(1), 11–28 (2014).
[47]D. Scott, C. M. Hall, and S. Gössling, "A review of the IPCC Fifth Assessment and implications for tourism sector climate resilience and decarbonization," J. Sustainable Tourism **24**(1), 8–30 (2016).
[48]S. E. Werners, E. Sparkes, E. Totin, N. Abel, S. Bhadwal, J. R. Butler *et al.*, "Advancing climate resilient development pathways since the IPCC's fifth assessment report," Environ. Sci. Policy **126**, 168–176 (2021).
[49]D. Jiang, Y. Sui, and X. Lang, "Timing and associated climate change of a 2 °C global warming," Int. J. Climatol. **36**(14), 4512–4522 (2016).
[50]R. J. Nicholls and A. Cazenave, "Sea-level rise and its impact on coastal zones," Science **328**(5985), 1517–1520 (2010).
[51]P. Huang and J. Ying, "A multimodel ensemble pattern regression method to correct the tropical Pacific SST change patterns under global warming," J. Clim. **28**(12), 4706–4723 (2015).
[52]X. Chen and T. Zhou, "Distinct effects of global mean warming and regional sea surface warming pattern on projected uncertainty in the South Asian summer monsoon," Geophys. Res. Lett. **42**(21), 9433–9439, https://doi.org/10.1002/2015GL066384 (2015).
[53]V. Echevin, M. Gévaudan, D. Espinoza-Morriberón, J. Tam, O. Aumont, D. Gutierrez *et al.*, "Physical and biogeochemical impacts of RCP8.5 scenario in the Peru upwelling system," Biogeosciences **17**(12), 3317–3341 (2020).
[54]J. K. Moore, K. Lindsay, S. C. Doney, M. C. Long, and K. Misumi, "Marine ecosystem dynamics and biogeochemical cycling in the Community Earth System Model [CESM1 (BGC)]: Comparison of the 1990s with the 2090s under the RCP4.5 and RCP8.5 scenarios," J. Clim. **26**(23), 9291–9312 (2013).
[55]M. A. Bender, T. R. Knutson, R. E. Tuleya, J. J. Sirutis, G. A. Vecchi, S. T. Garner *et al.*, "Modeled impact of anthropogenic warming on the frequency of intense Atlantic hurricanes," Science **327**(5964), 454–458 (2010).
[56]Y. Meng, M. Matsui, and K. Hibi, "An analytical model for simulation of the wind-field in a typhoon boundary-layer," J. Wind Eng. Ind. Aerodyn. **56**(2–3), 291–310 (1995).
[57]W. F. Huang and Y. L. Xu, "A refined model for typhoon wind field simulation in boundary layer," Adv. Struct. Eng. **15**(1), 77–89 (2012).
[58]W. F. Huang, Y. L. Xu, C. W. Li, and H. J. Liu, "Prediction of design typhoon wind speeds and profiles using refined typhoon wind field model," Adv. Steel Constr. **7**(4), 387–402 (2011).
[59]R. A. Fisher and L. H. C. Tippett, "Limiting forms of the frequency distribution of the largest or smallest member of a sample," Math. Proc. Cambridge Philos. Soc. **24**, 180–190 (1928).
[60]E. J. Gumbel, *Statistics of Extremes* (Columbia University Press, 1958).
[61]L. Weiss, "Asymptotic inference about a density function at an end of its range," Naval Res. Logist. Q. **18**(1), 111–114 (1971).

[62]E. Simiu and N. Heckert, "Extreme wind distribution tails: A 'peaks over threshold' approach," J. Struct. Eng. **122**(5), 539–547 (1996).
[63]Y. An and M. Pandey, "A comparison of methods of extreme wind speed estimation," J. Wind Eng. Ind. Aerodyn. **93**(7), 535–545 (2005).
[64]N. Cook, "Towards better estimation of extreme winds," J. Wind Eng. Ind. Aerodyn. **9**(3), 295–323 (1982).
[65]J. D. Holmes, P. Hitchcock, K. Kwok, and J. Chim, "Re-analysis of typhoon wind speeds in Hong Kong," in Fifth Asia-Pacific Conference on Wind Engineering, Kyoto, Japan, 2001.
[66]J. D. Holmes, K. Kwok, and P. A. Hitchcock, "Extreme wind speeds and wind load factors for Hong Kong," in The Seventh Asia-Pacific Conference on Wind Engineering, 2009.
[67]Y. Liu, D. Chen, S. Li, P. W. Chan, and Q. Zhang, "A three-dimensional numerical simulation approach to assess typhoon hazards in China coastal regions," Nat. Hazards **96**(2), 809–835 (2019).
[68]S. Soisuvarn and S. Oudomying, "Characterization of the tropical cyclones wind radii in the North Western Pacific Basin using the ASCAT winds data products," in *Progress in Electromagnetics Research Symposium (PIERS-Toyama)* (IEEE, 2018).
[69]G. Fang, L. Zhao, S. Cao, L. Zhu, and Y. Ge, "Estimation of tropical cyclone wind hazards in coastal regions of China," Nat. Hazards Earth Syst. Sci. **20**(6), 1617–1637 (2020).
[70]S. Nayak and T. Takemi, "Robust responses of typhoon hazards in northern Japan to global warming climate: Cases of landfalling typhoons in 2016," Meteorol. Appl. **27**(5), e1954 (2020).
[71]T. C. Wu, C. S. Velden, S. J. Majumdar, H. Liu, and J. L. Anderson, "Understanding the influence of assimilating subsets of enhanced atmospheric motion vectors on numerical analyses and forecasts of tropical cyclone track and intensity with an ensemble Kalman filter," Mon. Weather Rev. **143**(7), 2506–2531 (2015).
[72]P. Duran and J. Molinari, "Upper-tropospheric low Richardson number in tropical cyclones: Sensitivity to cyclone intensity and the diurnal cycle," J. Atmos. Sci. **73**(2), 545–554 (2016).
[73]R. J. Stouffer, V. Eyring, G. A. Meehl, S. Bony, C. Senior, B. Stevens *et al.*, "CMIP5 scientific gaps and recommendations for CMIP6," Bull. Am. Meteorol. Soc. **98**(1), 95–105 (2017).
[74]S. Kanada, S. Tsujino, H. Aiki, M. K. Yoshioka, Y. Miyazawa, K. Tsuboki *et al.*, "Impacts of SST patterns on rapid intensification of Typhoon Megi (2010)," J. Geophys. Res.: Atmos. **122**(24), 13,245–13,262, https://doi.org/10.1002/2017JD027252 (2017).
[75]J. C. L. Chan and K. S. Liu, "Global warming and western North Pacific typhoon activity from an observational perspective," J. Clim. **17**(23), 4590–4602 (2004).
[76]Y. Liu, S. Li, P. W. Chan, and D. Chen, "Empirical correction ratio and scale factor to project the extreme wind speed profile for offshore wind energy exploitation," IEEE Trans. Sustainable Energy **9**(3), 1030–1040 (2018).
[77]I. Lin and J. C. Chan, "Recent decrease in typhoon destructive potential and global warming implications," Nat. Commun. **6**(1), 7182 (2015).
[78]W. S. Ho and S. Ying, "An epidemiological study of 1063 hospitalized burn patients in a tertiary burns centre in Hong Kong," Burns **27**(2), 119–123 (2001).
[79]E. C. Chow, R. C. Li, and W. Zhou, "Influence of tropical cyclones on Hong Kong air quality," Adv. Atmos. Sci. **35**(9), 1177–1188 (2018).